Constrained Nonlinear and Mixed Effects Differential Equation Models for Dynamic Cell Polarity Signaling

Zhen Xiao
Biogen Inc.
Cambridge, MA 02142, USA

Nicolas Brunel
ENSIIE & Laboratoire de Mathématiques et Modélisation d'Evry
UMR CNRS 8071, Universite d'Evry, France.

Zhenbiao Yang
Center for Plant Cell Biology, Botany and Plant Sciences Department
University of California, Riverside, CA 92521, USA

Xinping Cui*
Department of Statistics
University of California, Riverside, CA 92521, USA
email: xinping.cui@ucr.edu

May 3, 2016

Author's Footnote:

Zhen Xiao was a PhD student in the Department of Statistics at University of California, Riverside. He is now a senior biosatistician at Biogen Inc, Cambridge, MA, 02142 (email: nehzxiao@gmail.com); and Nicolas Brunel is an associate professor in ENSIIE & Laboratoire de Mathématiques et Modélisation d'Evry UMR CNRS 8071, Universite d'Evry, France (email: nicolas.brunel@ensiie.fr); and Zhenbiao Yang is a professor in the Department of Botany and Plant Sciences and the Center for Plant Cell Biology and Institute for Integrative Genome Biology at University of California, Riverside, CA 92521, USA (email: zhenbiao.yang@ucr.edu); and Xinping Cui is a professor in the Department of Statistics and the Center for Plant Cell Biology and Institute for Integrative Genome Biology at University of California, Riverside, CA 92521, USA (email: xinping.cui@ucr.edu). This work was partially supported by UC Riverside AES-CE RSAP A01869.

Abstract

The key of tip growth in eukaryotes is the polarized distribution on plasma membrane of a particle named ROP1. This distribution is the result of a positive feedback loop, whose mechanism can be described by a Differential Equation parametrized by two meaningful parameters k_{pf} and k_{nf}. We introduce a mechanistic Integro-Differential Equation (IDE) derived from a spatiotemporal model of cell polarity and we show how this model can be fitted to real data i.e. ROP1 intensities measured on pollen tubes. At first, we provide an existence and uniqueness result for the solution of our IDE model under certain conditions. Interestingly, this analysis gives a tractable expression for the likelihood, and our approach can be seen as the estimation of a constrained nonlinear model. Moreover, we introduce a population variability by a constrained nonlinear mixed model. We then propose a constrained Least Squares method to fit the model for the single pollen tube case, and two methods, constrained Methods of Moments and constrained Restricted Maximum Likelihood (REML) to fit the model for the multiple pollen tubes case. The performances of all three methods are studied through simulations and are used on an in-house multiple pollen tubes dataset generated at UC Riverside.

Keywords: Constrained Mixed effects model, Restricted maximum likelihood, Semilinear-linear Elliptic Differential Equation, Integro-Differential Equation, Cell Polarity.

1. INTRODUCTION

Cell polarity is a fundamental feature of almost all cells. It is required for the differentiation of new cells, the formation of cell shapes, and cell migration, etc. Pollen tubes, which extend by an extreme form of polar growth (termed tip growth) to deliver sperms to the ovary for fertilization, are one of the fastest growing cells in plants and therefore represent an attractive model system to investigate polarized cell growth (Yang, 1998; Hepler et al., 2001; Lee and Yang, 2008; Yang, 2008; Qin and Yang, 2011).

When pollen grain is activated by a certain internal or external stimulus, the signaling molecule GTPase ROP1 in the cytosol will be activated and translocated onto the plasma membrane, forming an apical ROP1 cap. Once maintained, the apical ROP1 cap will trigger exocytosis, leading to cell growth at the site of the apical cap. Figure 1 shows the three main stages of pollen tube tip growth: polarity establishment of the signaling molecule GTPase ROP1 (i.e, active ROP1s form a apical cap), exocytosis to increase cell membrane surface and deliver cell wall materials, and cell wall extension.

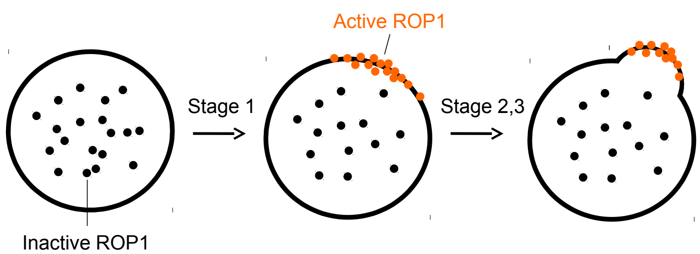

Figure 1: Three main stages of tip growth of pollen tubes. Stage 1: ROP1 polarity establishment; Stage 2: Pectin Exocytosis; Stage 3: Cell wall extension.

Several mathematical models have been built to simulate pollen tube tip growth (Dumais et al., 2006; J. H. Kroeger, 2008; Campas and Mahadevan, 2009; Lowery and Vanvactor, 2009; Fayant et al., 2010). These models focused on the cell wall mechanics and the cell wall mechanics-mediated shape formation of pollen tubes. However, it has been found that the generation of apical cap of active ROP1 at stage 1 plays a predominant role in determining polarity of the pollen tube (Lin et al., 1996; Li et al., 1998). Therefore, modeling the distribution of ROP1s on the membrane is the key to understand the tip growth of pollen tube. As a key regulator of the self-organizing pollen tube system, the activity and distribution of ROP1 are fine-tuned by both positive and negative feedback mechanisms (Hwang et al., 2010) as well as slow diffusion shown in Figure 2. Altschuler et al. (2008) proposed a linear differential equation model for the polarization of the GTPase Cdc42 in budding yeast but only considered positive feedback. On the other hand, for all the aforementioned models attention has been paid to predict or simulate the output using these models with given parameters. Less efforts have been devoted to the inverse problem, i.e., using the experimental data to estimate the parameters that characterize these models (Ramsay et al., 2007; Wu and Chen, 2008; Brunel, 2008; Brunel et al., 2014).

In this paper, we propose an integro-ordinary differential equation (IDE) model to describe the three processes together (positive feedback, negative feedback and diffusion) that lead to ROP1 polarity formation at steady state. Our main interest lies in the inverse problem of estimating the parameters for the positive feedback and the negative feedback. However, two identifiability issues arise in the context of our model. The first identifiability problem is whether the solution to the nonlinear IDE model exists and is unique. We will show that the IDE model is closely related to a semilinear elliptic equation, from which we establish the original theory on the existence and uniqueness of solutions to this type of IDE. The second identifiability problem is whether the observed data is enough to identify the parameters in the IDE model. By applying the identifiability analysis methods suggested by Miao et al. (2011), we can prove that the two parameters of interest are identifiable.

Solving the identifiability problems allows us to derive an admissible parameter space inside which the solution to the IDE model exists. The IDE model can then be re-parametrized as a mixed-effects differential equation model with linear constraints over the admissible parameter space. In statistical literature, there exist a number of papers for mixed-effects differential equation models. Li et al. (2002) proposed to estimate time-varying parameters in the mixed-effects ordinary differential equations by maximizing the double penalized log likelihood. Putter et al. (2002) proposed a hierarchical Bayesian approach for estimating population parameters in a system of mixed-effects nonlinear differential equations that have closed-form solutions. Guedj et al. (2007) extended this system of mixed-effects nonlinear differential equations for which no closed form is available. They proposed to estimate both population and individual parameters in this extended model by a maximum likelihood approach using a Newton-like algorithm. Huang and Wu (2006a) and Huang and Wu (2006b) developed a hierarchical Bayesian approach to estimate both population and individual dynamic parameters in a set of mixed-effects nonlinear differential equations which have no closed-form solutions. Lu et al. (2011) employed stochastic approximation EM approach for parameter estimation of mixed-effects ordinary differential equations.

However, parameter estimation problems for mixed-effects differential equation models with linear inequality constraints have not been investigated. In this paper, we propose two algorithms based on modified REML and Method of Moments (MM) approaches (Lu and Meeker, 1993) to estimate the parameters with constraints in a mixed-effects differential equation model. The constrained estimators are shown to be consistent and the methodology we propose is quite general and can be applied to many mixed-effects ODE settings with little modification.

The paper is organized as follows. In section 2, we introduce the IPDE and IDE model motivated by the GTPbase ROP1 polarization process. In the next section, we give sufficient and necessary conditions for existence and uniqueness of a positive solution to the IDE model, and we derive a tractable generic expression for solutions of the IDE. In section 4, we introduce the IDE based nonlinear statistical model with linear constraint for a single pollen tube. We then extend the model for multiple pollen tubes and re-parametrize it as a nonlinear mixed model with linear constraints. The two estimators of Constrained Method of Moments (CMM) and Constrained REML(CREML) are proposed and the asymptotic properties of CMM are discussed. We examine the performance of the proposed estimation procedures through simulation studies in section 5 and real data analysis in section 6. We conclude the paper in section 7.

2. AN INTEGRAL-DIFFERENTIAL EQUATION MODEL OF CELL POLARITY

To build the cell-signaling model of ROP1 polarity formation and maintenance, we assume that the redistribution of signaling molecules is determined by three fundamental transport mechanisms including (1) A positive feedback loop with rate k_{pf} mediated by exocytosis and ROP1 activators such as RopGEFs (Kost et al., 1999; Li et al., 1999; Berken et al., 2005; Gu et al., 2005; Lee et al., 2008; McKenna et al., 2009); (2) A global negative regulation with rate k_{nf} mediated by cytosolic

ROP1 inhibitors such as RopGAPs (Hwang et al., 2008); (3) Slow lateral diffusion of ROP1 protein on apical plasma membrane with rate D. These three processes are shown in Figure 2. The following semilinear Integro-Partial Differential Equation describes how these three processes together lead to ROP1 polarity formation:

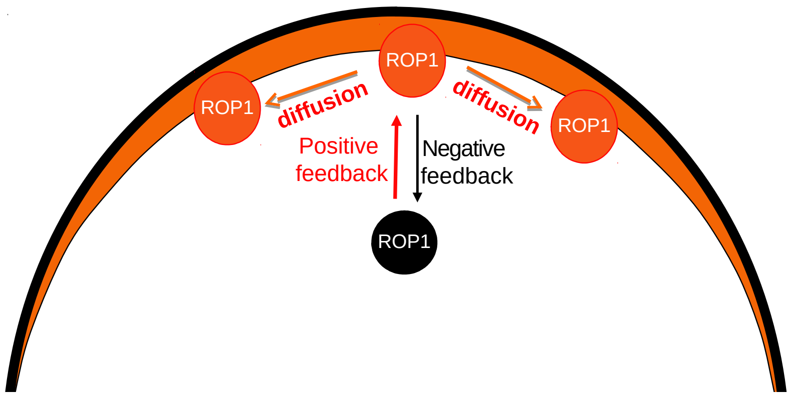

Figure 2: ROP1 polarity formation is determined by positive feedback, negative feedback and lateral diffusion process.

$$\begin{cases} \frac{\partial R(x,t)}{\partial t} = k_{pf} R(x,t)^{\alpha} \left(1 - \frac{\int_{-L_0}^{L_0} R(x,t)dx}{R_{tot}}\right) - k_{nf} R(x,t) + D\nabla^2 R(x,t) \\ \text{where} \qquad \{x,t\} \in [-L_0, L_0] \times [0,\infty], \qquad R(-L_0,t) = R(L_0,t) = 0 \end{cases} \tag{1}$$

$R(x,t)$ denotes the ROP1 intensity in position x on the membrane at time t, which can be observed at a oblique plane of total length $2L_0$ passing through the cell center. R_{tot} denotes the total free ROP1 in the cell. Throughout this paper, R_{tot}, D, $\alpha > 1$ and L_0 are assumed to be known constants. This model is similar as the PDE model described in Altschuler et al. (2008) except in their model spontaneous association was included, the fraction of all particles on the membrane is specified as $\frac{\int_{-L_0}^{L_0} R(x,t)dx}{R_{tot}}$ and α was assumed to be 1.

At equilibrium t_0, $\frac{\partial R(x,t)}{\partial t}|_{t=t_0} = 0$, *i.e.*, the ROP1 density won't change with time. From now on, we write $R(x,t_0)$ as $R(x)$. The IPDE model (1) then degenerates to the following IDE model

$$\begin{cases} -D\partial_x^2 R = -k_{nf} R + k_{pf} R^{\alpha} \left(1 - \frac{\int_{-L_0}^{L_0} R dx}{R_{tot}}\right) \\ \text{where} \qquad x \in [-L_0, L_0], \qquad R(-L_0) = R(L_0) = 0 \end{cases} \tag{2}$$

Our interest lies in the estimation of the parameters for k_{pf} and k_{nf}. However, two issues immediately arise, namely, the existence and uniqueness of the solution R to the equation (2) and the identifiability of k_{pf} and k_{nf}. Section 3 is devoted to address these two issues.

3. IDENTIFIABILITY ANALYSIS

In this section, we first show that the solution R to the equation (2) exists and is unique. To the best of our knowledge, this is the first study on the existence and uniqueness of solution to integral differential equations when $\alpha \geq 1$. We then apply the identifiability analysis suggested by Miao et al. (2011) and verified that parameters k_{pf} and k_{nf} are identifiable.

3.1 Existence and Uniqueness of Solution R

Lemma 1. *For all $c \in (0, \infty]$, there exists an unique positive solution $\sigma_0(x)$ to (3) with Dirichlet conditions on $[-c, c]$.*

$$\begin{cases} -\partial_x^2 u = -u + u^\alpha \quad x \in [-c, c] \\ u(-c) = u(c) = 0 \end{cases} \tag{3}$$

Moreover, $\sigma_0(x)$ is positive, even and increasing at $[-c, 0]$ and decreasing at $[0, c]$.

Lemma 2. *For all $\lambda^{'} > 0$, there exists an unique positive solution $R_{\lambda'}(x)$ to (4) with Dirichlet conditions on $\Omega = [-L_0, L_0]$, where $L_0 \in (0, \infty]$.*

$$\begin{cases} -D\partial_x^2 u = -k_{nf}u + \lambda' k_{pf} u^\alpha \\ where \qquad x \in [-L_0, L_0], \qquad u(-L_0) = u(L_0) = 0 \end{cases} \tag{4}$$

Moreover, if $\sigma_0(x)$ is the unique positive solution to (3) defined on $\Omega' = \left[-L_0\sqrt{\frac{k_{nf}}{D}}, L_0\sqrt{\frac{k_{nf}}{D}}\right]$, then

$$R_{\lambda'}(x) = \left(\frac{k_{pf}}{k_{nf}}\lambda'\right)^{\frac{1}{1-\alpha}} \sigma_0(\sqrt{\frac{k_{nf}}{D}}x) \doteq R_{\lambda,\mu}(x) = \lambda\sigma_0(\mu x). \tag{5}$$

Where $\lambda = (\frac{k_{pf}}{k_{nf}}\lambda')^{\frac{1}{1-\alpha}}$, and $\mu = \sqrt{\frac{k_{nf}}{D}}$.

The proofs of Lemma 1 and 2 are provided in the Appendix. It is easy to see that if there exists a unique positive solution $R_{\lambda'}(x)$ to equation (4) such that $\lambda^{'} = 1 - \frac{\int_x R_{\lambda'}(x)dx}{R_{tot}}$, then $R_{\lambda'}(x)$ is also a solution to equation (2). In the following, we provide sufficient and necessary conditions that solutions to equation (4) are also solutions to equation (2).

Sufficient Condition: Let σ_0 be the positive solution to (3) on $\Omega' = \left[-L_0\sqrt{\frac{k_{nf}}{D}}, L_0\sqrt{\frac{k_{nf}}{D}}\right]$. Consider the family of function $R_{\lambda,\mu}(x)$ defined in (5) and the discriminant function

$$\Lambda(k_{nf}, k_{pf}, D, R_{tot}, \sigma_0) = \frac{k_{nf}}{k_{pf}} - \frac{1}{\alpha}\left(\frac{\alpha-1}{\alpha}\sqrt{\frac{k_{nf}}{D}}\frac{R_{tot}}{\|\sigma_0\|_1}\right)^{\alpha-1} \tag{6}$$

If $\Lambda(k_{nf}, k_{pf}, D, R_{tot}, \sigma_0) = 0 (< 0)$, then one (two) positive solution(s) to (2) can be found in the family of function $R_{\lambda,\mu}(x)$.

Necessary Condition: Any positive solution to (2) can be written in the form $R_{\lambda,\mu}(x) = \lambda\sigma_0(\mu x)$.

Remark 1. *The proofs of sufficient condition and necessary condition are provided in the Appendix. As a result, the solution R to (2) can be obtained as following when the values of k_{nf} and k_{pf} are given*

1. *Solve the semilinear elliptic equation (3) on* $\Omega' = \left[-L_0\sqrt{\frac{k_{nf}}{D}}, L_0\sqrt{\frac{k_{nf}}{D}}\right]$.
2. *Compute* $\|\sigma_0\|_1$ *and the discriminant function* $\Lambda(k_{nf}, k_{pf}, D, R_{tot}, \sigma_0)$.
3. *If* $\Lambda(k_{nf}, k_{pf}, D, R_{tot}, \sigma_0) = 0$*, find the positive roots* λ^* *of* $g(\lambda)$ *(defined in the Appendix section A.3), and compute the solution* $R_{\lambda^*,\mu}(x)$.
4. *If* $\Lambda(k_{nf}, k_{pf}, D, R_{tot}, \sigma_0) < 0$*, find the positive roots* λ_1^* *and* λ_2^* *of* $g(\lambda)$ *(defined in the Appendix section A.3), and compute the solutions* $R_{\lambda_1^*,\mu}(x)$ *and* $R_{\lambda_2^*,\mu}(x)$.

In practice, the solution closer to the experimental data should be chooen if there are two solutions.

Remark 2. *For $\lambda > 0$, the solution $R_{\lambda,\mu}(x)$ to (2) is a positive and even function. Moreover, it increases at $[-L_0, 0]$ and decreases at $[0, L_0]$, and the maximum $R_{\lambda,\mu}(0) = \max_{x\in\Omega} R_{\lambda,\mu}(x) > \lambda$. The proof is provided in the Appendix. It will be shown later in section 7 that the ROP data reflects these qualitative properties.*

Remark 3. *From sufficient condition, we see that the solution of (2) is determined by two parameters, μ and λ, which can be seen as a reparametrization of k_{nf} and k_{pf}. Hence, (2) is not over parametrized by k_{nf} and k_{pf}.*

3.2. Identifiability of k_{nf} and k_{pf}

In this section, we prove that the parameters of interest k_{nf} and k_{pf} are globally identifiable and therefore are locally strongly identifiable.

Let $R(x)$ denote the solution to (2). In practice, $R(x)$ is a positive and non-constant function on interval $[-L_0, L_0] \subset [-L, L]$. Suppose for parameters (k^0_{nf}, k^0_{pf}) and (k^1_{nf}, k^1_{pf}), $R(x; k^0_{nf}, k^0_{pf}) = R(x; k^1_{nf}, k^1_{pf})$ on $[-L_0, L_0]$, then we have

$$k^0_{nf}R(x) - k^0_{pf}R^{\alpha}(x)\left(1 - \frac{\int_{-L}^{L} R(x)dx}{R_{tot}}\right) = k^1_{nf}R(x) - k^1_{pf}R^{\alpha}(x)\left(1 - \frac{\int_{-L}^{L} R(x)dx}{R_{tot}}\right)$$

For $R(x) > 0$ on $[-L_0, L_0]$

$$k^0_{nf} - k^1_{nf} = (k^0_{pf} - k^1_{pf})R^{\alpha-1}(x)\left(1 - \frac{\int_{-L}^{L} R(x)dx}{R_{tot}}\right)$$

If $k^0_{pf} - k^1_{pf} \neq 0$, then

$$R^{\alpha-1}(x) = (k^0_{nf} - k^1_{nf}) \Big/ \left((k^0_{pf} - k^1_{pf})\left(1 - \frac{\int_{-L}^{L} R(x)dx}{R_{tot}}\right)\right),$$

suggesting that $R(x)$ has to be constant on $[-L_0, L_0]$ since $1 - \frac{\int_{-L}^{L} R(x)dx}{R_{tot}} > 0$. By contradiction, we can show that $k^0_{pf} - k^1_{pf} = 0$ and $k^0_{nf} - k^1_{nf} = 0$, i.e., $R(x; k^0_{nf}, k^0_{pf}) = R(x; k^1_{nf}, k^1_{pf})$ on $[-L_0, L_0]$ if and only if $k^0_{pf} = k^1_{pf}$ and $k^0_{nf} = k^1_{nf}$.

4. PARAMETER ESTIMATION

In this section, we first consider estimating k_{nf} and k_{pf} in a constrained nonlinear fixed effect model using a single pollen tube data. We then further extend to estimate k_{nf} and k_{pf} in a constrained nonlinear mixed effect model using multiple pollen tube data.

4.1 Single pollen tube and constrained nonlinear fixed effect model

Suppose for a single pollen tube, an observation of ROP1 intensity in a position X_j (X_j is randomly sampled from known distribution $F(x)$ such as an uniform distribution) on the membrane at equilibrium t_0 is denoted by

$$Y_j = R(X_j; k_{nf}, k_{pf}) + \epsilon_j \qquad j = 1, 2, \cdots, n. \tag{7}$$

where $R(X;\cdot)$ is the solution of (2) and ϵ_j are *iid* from a certain distribution f with mean 0 and variance σ^2. As shown in section 2, $R(X;\cdot)$ exists if and only if the discriminant function $\Lambda(\cdot)$ is non-positive. Therefore, the IDE based model (7) is subject to the constraint

$$\begin{cases} \Lambda(k_{nf}, k_{pf}, D, R_{tot}, \sigma_0) = \frac{k_{nf}}{k_{pf}} - \frac{1}{\alpha}\left(\frac{\alpha-1}{\alpha}\sqrt{\frac{k_{nf}}{D}}\frac{R_{tot}}{\|\sigma_0\|_1}\right)^{\alpha-1} \leq 0 \\ k_{nf} > 0, k_{pf} > 0 \end{cases}$$

Proposition 1. *The constrained nonlinear model (7) can be reparametrized into the following model (8) with μ and λ subject to the constraint (9)*

$$Y_j = \lambda\sigma_0(\mu X_j) + \epsilon_j. \tag{8}$$

$$\begin{cases} \Lambda^*(\mu, \lambda) = \mu R_{tot} - \lambda \|\sigma_0\|_1 > 0 \\ \mu > 0, \lambda > 0 \end{cases} \tag{9}$$

where $\mu = \sqrt{\frac{k_{nf}}{D}}$ and λ is the root of $g(\lambda)$ (defined in the Appendix section A.3). The choice of λ is discussed in Remark 1.

The proof of proposition 1 is provided in the Appendix. As a result, given the observations $\{y_j\}_{j=1}^n$ at positions $\{x_j\}_{j=1}^n$ from the biological experiment, we propose the following estimation method called Constrained Nonlinear Least Square (CNLS) method.

1. Compute $\sigma_0(x)$ from DE (3)

2. Estimate μ and λ by minimizing (10) under the constraint (9)

$$(\hat{\lambda}, \hat{\mu}) = \arg\min_{\lambda,\mu} \sum_{j=1}^{n} (y_j - \lambda\sigma_0(\mu x_j))^2 \tag{10}$$

3. Convert $\hat{\mu}$ and $\hat{\lambda}$ to $\hat{k}_{nf}$ and $\hat{k}_{pf}$ by $\hat{k}_{nf} = D\hat{\mu}^2$ and $\hat{k}_{pf} = \frac{D\hat{\mu}^2}{\hat{\lambda}^{\alpha-1} - \frac{\hat{\lambda}^{\alpha}\|\sigma_0\|_1}{\hat{\mu}R_{tot}}}$

4. Estimate σ^2 by $\hat{\sigma}^2 = \frac{1}{n}\sum_{j=1}^{n}\left(y_j - \hat{\lambda}\sigma_0(\hat{\mu}x_j)\right)^2$

In the first step of CNLS, the solution of σ_0 involves a boundary value problem in an ordinary differential equation, which can be solved by many methods including shooting method (Soetaert, 2009; Soetaert et al., 2010), mono-implicit Runge-Kutta (MIRK) method (Cash and Mazzia, 2005) and collocation method (Bader and Ascher, 1987) in R package “bvpSolve”. The optimization in the second step is subject to one linear constraint and two box constraints. When there is no constraint, the optimization can be tackled by many gradient based methods which require the objective function to be differentiable, such as the Newton method, the BFGS method, the Gauss-Newton method, etc. On the other hand, the simplex method (Nelder and Mead, 1965) that directly searches the optimum allows the objective function to be not differentiable. To apply the simplex method, we first incorporate the constraints into the objective function by defining

$$f(\mu, \lambda) = \begin{cases} \sum_{j=1}^{n} (y_j - \lambda\sigma_0(\mu x_j))^2 & \text{if } \Lambda^*(\mu, \lambda) > 0 \text{ and } \mu > 0 \text{ and } \lambda > 0 \\ +\infty & o.w. \end{cases}$$

The same idea was used by Nelder and Mead (1965).

For the general Nonlinear Least Square (NLS) estimator, the asymptotic properties have been established by Jennrich (1969). For the general Constrained NLS (CNLS) estimator, the asymptotic properties have been established by Wang (1996). Below we present the asymptotic properties of the CNLS estimator proposed in this paper. The proof is provided in the Appendix.

Proposition 2. *Let $\boldsymbol{\theta} = (\mu, \lambda)^T$ be the parameter vector, $\boldsymbol{\theta}_0$ be the true value of $\boldsymbol{\theta}$, and $\hat{\boldsymbol{\theta}}_n$ be the CNLS estimator with n sample points. Let $R(X; \boldsymbol{\theta}) = \lambda\sigma_0(\mu X)$, then*

$$\sqrt{n}(\hat{\boldsymbol{\theta}}_n - \boldsymbol{\theta}_0) \xrightarrow{d} N(0, \sigma^2 K^{-1})$$

where $K = E_X[\nabla_{\boldsymbol{\theta}} R(X; \boldsymbol{\theta}_0) \nabla_{\boldsymbol{\theta}} R(X; \boldsymbol{\theta}_0)^T]$, and $\nabla_{\boldsymbol{\theta}} R(X; \boldsymbol{\theta}_0)$ is the gradient vector of $R(X; \boldsymbol{\theta})$ with respect to $\boldsymbol{\theta}$ at $\boldsymbol{\theta} = \boldsymbol{\theta}_0$.

Proposition 3. *Let the estimate of σ^2 be $\hat{\sigma}_n^2 = \frac{1}{n} \sum_{j=1}^{n} \left(y_j - \hat{\lambda}\sigma_0(\hat{\mu} x_j) \right)^2$. Then*

$$\hat{\sigma}_n^2 \xrightarrow{p} \sigma^2$$

Then by Slutsky's Theorem

$$\frac{\sqrt{n}(\hat{\boldsymbol{\theta}}_n - \boldsymbol{\theta}_0)}{\hat{\sigma_n}} \xrightarrow{d} N(0, K^{-1})$$

Corollary 1. *Denote $\boldsymbol{\phi} = (k_{nf}, k_{pf})^T$. Let $\boldsymbol{\phi}_0$ and $\hat{\boldsymbol{\phi}}_n$ be the true value and estimator of $\boldsymbol{\phi}$ respectively, where $\hat{k}_{nf} = D\hat{\mu}^2$ and $\hat{k}_{pf} = \dfrac{D\hat{\mu}^2}{\hat{\lambda}^{\alpha-1} - \dfrac{\hat{\lambda}^{\alpha} \parallel \sigma_0 \parallel_1}{\hat{\mu} R_{tot}}}$. By the delta-method,*

$$\frac{\sqrt{n}(\hat{\boldsymbol{\phi}}_n - \boldsymbol{\phi}_0)}{\hat{\sigma_n}} \xrightarrow{d} N(0, A^T K^{-1} A)$$

where

$$A = \begin{pmatrix} \frac{\partial k_{nf}}{\partial \mu} & \frac{\partial k_{pf}}{\partial \mu} \\ \frac{\partial k_{nf}}{\partial \lambda} & \frac{\partial k_{pf}}{\partial \lambda} \end{pmatrix} = \begin{pmatrix} 2D\mu & \frac{2D\mu^3 - 3D\mu^2\lambda\frac{\|\sigma_0\|_1}{R_{tot}}}{\lambda^{\alpha-1}(\mu-\lambda\frac{\|\sigma_0\|_1}{R_{tot}})^2} \\ 0 & \frac{-D\mu^4(\alpha-1)+D\mu^3\alpha\lambda\frac{\|\sigma_0\|_1}{R_{tot}}}{\lambda^{\alpha}(\mu-\lambda\frac{\|\sigma_0\|_1}{R_{tot}})^2} \end{pmatrix}$$

4.2 Multiple pollen tubes and constrained nonlinear mixed effect model

In this section, we consider multiple pollen tubes and extend model 7 and 8 as follows:

$$Y_{ij} = R_i(X_{ij}; \lambda_i, \mu_i) + \epsilon_{ij} \tag{11}$$

$$= \lambda_i \sigma_0(\mu_i X_{ij}) + \epsilon_{ij}, \qquad i = 1, 2, \cdots, m; j = 1, 2, \cdots, n_i, \tag{12}$$

where Y_{ij} denotes the ROP1 intensity observed for pollen tube i at position X_{ij} on the membrane at static time and ϵ_{ij} is $i.i.d$ with distribution $N(0, \sigma^2)$. We further assume that

$$\begin{cases} (\mu_i, \lambda_i)^T = (\mu, \lambda)^T + \Phi_i \\ \lambda_i > 0, \quad \mu_i > 0 \end{cases} \tag{13}$$

where Φ_i is $i.i.d$ with distribution $MVN(0, \Sigma)$. As a result, this is a nonlinear mixed model (NMM) where σ^2 measures within pollen tube variation and Σ measures between pollen tube variation. As discussed in Section 4.1, each pair of $\lambda_i > 0, \mu_i$ are subject to three constraints. If no constraint exists, all the parameters can be estimated by several existing methods such as Ke and Wang (2001) and Wolfinger and Lin (1997).

Denote $\boldsymbol{\theta}_i = (\mu_i, \lambda_i)^T$ and $\boldsymbol{\theta} = (\mu, \lambda)^T$, and the experimental data to be $\{y_{ij}\}$ and $\{x_{ij}\}$ with $i = 1, \cdots, m$ and $j = 1, \cdots, n_i$. We first extend the CNLS procedure and propose a new procedure called Constrained Method of Moment (CMM) as follows:

1. Compute $\sigma_0(x)$ from equation (3)

2. For each pollen tube i, estimate $\boldsymbol{\theta}_i$ by minimizing least squares

$$\hat{\boldsymbol{\theta}}_i = \arg\min_{\boldsymbol{\theta}_i} \sum_{j=1}^{n_i} (y_{ij} - \lambda_i \sigma_0(\mu_i x_{ij}))^2$$

   under the constraints $\Lambda^*(\boldsymbol{\theta}_i) > 0$ and $\boldsymbol{\theta}_i > 0$

3. Estimate $\boldsymbol{\theta}$ by $\hat{\boldsymbol{\theta}} = \frac{\sum_{i=1}^m \hat{\boldsymbol{\theta}}_i}{m}$

4. Estimate σ^2 by $\hat{\sigma}^2 = \frac{\sum_{i=1}^{m}\sum_{j=1}^{n_i}\left(y_{ij}-\hat{\lambda}_i\sigma_0(\hat{\mu}_i x_{ij})\right)^2}{\sum_{i=1}^{m}(n_i-2)}$

5. Estimate Σ by $\hat{\Sigma} = \sum_{i=1}^{m}\frac{(\hat{\boldsymbol{\theta}}_i-\hat{\boldsymbol{\theta}})(\hat{\boldsymbol{\theta}}_i-\hat{\boldsymbol{\theta}})^T}{m-1} - \hat{\sigma}^2\sum_{i=1}^{m}\frac{T_i^{-1}}{m}$, where $T_i = \left[\frac{\partial \boldsymbol{R}_i}{\partial \boldsymbol{\theta}_i^T}\right]^T\left[\frac{\partial \boldsymbol{R}_i}{\partial \boldsymbol{\theta}_i^T}\right]\Bigg|_{\boldsymbol{\theta}_i=\hat{\boldsymbol{\theta}}_i}$ and $\boldsymbol{R}_i = (R(x_{i1};\boldsymbol{\theta}_i), R(x_{i2};\boldsymbol{\theta}_i), \cdots, R(x_{in_i};\boldsymbol{\theta}_i))^T$

6. Modify the estimator of Σ by

$$\Sigma^* = \begin{cases} \hat{\Sigma} & \text{if } \hat{\Sigma} \text{ is positive definite} \\ \hat{\Sigma}_+ & \text{if } \hat{\Sigma} \text{ is not positive definite} \end{cases}$$

where $\hat{\Sigma}_+ = Q\Psi_+Q'$, in which Ψ_+ is a diagonal matrix whose diagonal elements $\Psi_{ii} = max(\psi_i, 0)$ where ψ_i is the eigenvalue of Σ, and Q is a 2×2 matrix whose i^{th} columns is the eigenvector q_i associated with ψ_i.

7. Convert $\hat{\boldsymbol{\theta}}$ to $\hat{k}_{nf}$ and $\hat{k}_{pf}$

This procedure is motivated by the Method of Moments (MM) proposed by Lu and Meeker (1993). Our contribution is to extend it to constrained case by adding a constraint in the second step. Below we establish the asymptotic properties of the CMM estimators $\hat{\theta}$, Σ_{Φ}. The proof is provided in the Appendix.

Proposition 4. *Assume that*

1. *the sample size from each pollen tubes are equal, i.e.,* $n_1 = n_2 = \cdots = n_m = n$
2. *both* n *and* m *tend to* $+\infty$

Then, we have the following large sample properties for $\hat{\boldsymbol{\theta}}$

1. $\hat{\boldsymbol{\theta}} \xrightarrow{p} \boldsymbol{\theta}$
2. $\sqrt{m}\tilde{\Sigma}^{-\frac{1}{2}}(\hat{\boldsymbol{\theta}}-\boldsymbol{\theta}) \xrightarrow{d} \boldsymbol{Z}$, *where* $\boldsymbol{Z} \sim N(0, I_2)$, *and* $\tilde{\Sigma} = \Sigma + \sigma^2 E_{\boldsymbol{\theta}}[(nK_i)^{-1}]$ *with* $K_i = E_X[\nabla_{\boldsymbol{\theta}_i}R(X;\boldsymbol{\theta}_i)\nabla_{\boldsymbol{\theta}_i}R(X;\boldsymbol{\theta}_i)^T]$.

Moreover, if $\hat{\sigma}^2$ *is a consistent estimator of* σ^2*, then*

1. $\hat{\Sigma} \xrightarrow{p} \Sigma$

2. $\sqrt{m}\hat{\hat{\Sigma}}^{-\frac{1}{2}}(\hat{\boldsymbol{\theta}} - \boldsymbol{\theta}) \xrightarrow{d} \boldsymbol{Z}$*, where* $\hat{\hat{\Sigma}} = \hat{\Sigma} + \hat{\sigma}^2 E_{\boldsymbol{\theta}}[(nK_i)^{-1}]$*.*

Corollary 2. *Denote* $\boldsymbol{\phi} = (k_{nf}, k_{pf})^T$*. Let* $\boldsymbol{\phi}_0$ *and* $\hat{\boldsymbol{\phi}}$ *be the true value and estimator of* $\boldsymbol{\phi}$ *respectively. By the delta-method,*

$$\sqrt{m}(A^T\hat{\hat{\Sigma}}A)^{-\frac{1}{2}}(\hat{\boldsymbol{\phi}} - \boldsymbol{\phi}_0) \xrightarrow{d} \boldsymbol{Z}$$

where A *is given previously.*

Note that the CMM requires the same sample size among subjects, which is usually violated in real data. If ϵ_{ij} are *iid* normal, we can convert the nonlinear mixed model to a linear mixed model by Taylor approximation, and thereafter propose an alternative procedure called Constrained Restricted Maximum Likelihood method (CREML) as follows:

1. Given current Best Linear Unbiased Predictors (BLUP) $(\hat{\mu}_i^{(t)}, \hat{\lambda}_i^{(t)})$ for (μ_i, λ_i), use Taylor expansion to express $R_i(\mu_i, \lambda_i; x)$ as

$$R_i(\mu_i, \lambda_i; x) \approx R_i(\hat{\mu}_i^{(t)}, \hat{\lambda}_i^{(t)}; x) + \frac{\partial R_i}{\partial \mu_i}|_{\mu_i=\hat{\mu}_i^{(t)}}(\mu_i - \hat{\mu}_i^{(t)}) + \frac{\partial R_i}{\partial \lambda_i}|_{\lambda_i=\hat{\lambda}_i^{(t)}}(\lambda_i - \hat{\lambda}_i^{(t)})$$

As a result, the original expression of data $y_{ij} = R_i(\mu_i, \lambda_i; x_{ij}) + \epsilon_{ij}$ can be re-written as

$$\begin{aligned} y_{ij}^* &= \frac{\partial R_i}{\partial \mu_i}|_{\mu_i=\hat{\mu}_i^{(t)}}\mu_i + \frac{\partial R_i}{\partial \lambda_i}|_{\lambda_i=\hat{\lambda}_i^{(t)}}\lambda_i + \epsilon_{ij} \\ &= \begin{pmatrix} \frac{\partial R_i}{\partial \mu_i}|_{\mu_i=\hat{\mu}_i^{(t)}} \\ \frac{\partial R_i}{\partial \lambda_i}|_{\lambda=\hat{\lambda}_i^{(t)}} \end{pmatrix}^T \begin{pmatrix} \mu \\ \lambda \end{pmatrix} + \begin{pmatrix} \frac{\partial R_i}{\partial \mu_i}|_{\mu_i=\hat{\mu}_i^{(t)}} \\ \frac{\partial R_i}{\partial \lambda_i}|_{\lambda=\hat{\lambda}_i^{(t)}} \end{pmatrix}^T \Phi_i + \epsilon_{ij} \end{aligned} \tag{14}$$

where, $y_{ij}^* = y_{ij} - R_i(\hat{\mu}_i^{(t)}, \hat{\lambda}_i^{(t)}; x_{ij}) + \frac{\partial R_i}{\partial \mu_i}|_{\mu_i=\hat{\mu}_i^{(t)}}\hat{\mu}_i^{(t)} + \frac{\partial R_i}{\partial \lambda_i}|_{\lambda_i=\hat{\lambda}_i^{(t)}}\hat{\lambda}_i^{(t)}$, $\Phi_i \overset{iid}{\sim} MVN(0, \Sigma)$, $\epsilon_{ij} \overset{iid}{\sim} N(0, \sigma^2)$, $\Lambda^*(\mu, \lambda) = \mu R_{tot} - \lambda \parallel \sigma_0 \parallel_1 > 0$, $\lambda > 0$, $\mu > 0$. And our original model becomes a Constrained Linear Mixed Effect Model (CLMM).

2. Fit CLMM (14) under the constraints of $\Lambda^*(\mu, \lambda) > 0$, $\mu > 0$ and $\lambda > 0$. Such constraints at the population level can be easily embraced by REML.

3. Update $(\hat{\mu}_i^{(t)}, \hat{\lambda}_i^{(t)})$ by the Best Linear Unbiased Predictors (BLUP) based on the Best Linear Unbiased Estimates (BLUE) $(\hat{\mu}, \hat{\lambda}, \hat{\Sigma}, \hat{\sigma}^2)$ of the CLMM (14) from step 2.

4. Iterate the above three steps until convergence.

This procedure is motivated by the iterative procedure of Lindstrom and Bates (1990). Our contribution is to extend it to constrained case by adding a constraint on Step 2 and to use a simple way to update $(\hat{\mu}_i^{(t)}, \hat{\lambda}_i^{(t)})$ in the iteration process.

The convergence behavior of the CREML procedure depends on the starting value. A good choice of starting value could be the estimates of the CMM procedure. If no constraints exist, the CLMM model in step 2 can be fitted by many existing approaches such as MLE, REML and EM algorithm. In this paper, we consider REML and extend it to fit the model with constraints. Note that the likelihood in the first step of REML only involves the variance component parameters Σ and σ^2, therefore their estimates won't be affected by the constraints. On the other hand, the likelihood in the second step of REML involves the population parameters μ and λ. So their estimates should be obtained by maximizing the reduced likelihood under the constraints. And this constrained maximization problem was discussed in the previous section of single pollen tube case.

Note that the CMM procedure controls the constraints at the individual level whereas the CREML procedure controls them at the population level. Since constraints satisfied at the individual level will be automatically satisfied at the population level, the former is more strict than the latter. In many cases of real world application especially when the number of pollen tubes, m is large, constraints at the population level is more desirable.

5. SIMULATION STUDIES

In this section, simulation studies were conducted for the cases of single pollen tube and multiple pollen tubes respectively. All the estimation procedures were implemented in R. From the proof of Remark 2, we know $\sigma_0(x)$ is a positive and even function that achieves its maximum at 0. Further, we know $\sigma_0(x)$ is close to $\frac{1}{2}$ when $|x| = 5$ and is close to 0 when $|x| \geq 15$. Therefore, when $\mu = 1$, $R(x) = \lambda\sigma_0(\mu x)$ is close to 0 when $|x| \geq 15$. Therefore, in the simulation the data of $R(x)$ for $\mu = 1$ were generated from $|x| < 15$. The values of α, D and R_{tot} used in the simulations were set to be 1.2, 0.1 and 797 respectively, which were obtained empirically from real data.

5.1 Single pollen tube

To evaluate the performance of the CNLS procedure, we simulated data based on Remark 1 using the true values $k_{nf} = 0.1$, $k_{pf} = 0.1125$.Therefore, $\mu = 1$ and $\lambda = 34.1883$. Since the range of $R(x)$ is $[0, 55.06]$, we set the true value of measurement error σ to be 4, 8, 16. For different σ, we generated 10000 data sets of size $n = 301$, i.e., x were picked along $[-15, 15]$ with step size 0.1. CNLS based estimates of the parameters were obtained for each of the 10000 data sets, based on which the relative bias, standard deviation were computed as shown in Table 1. From Table 1, we could see the CNLS procedure works quite well and is quite robust against noise when the size of data is fairly large. We also followed Proposition 3 to compute asymptotical variances and construct the coverage probability as shown in Table 1. $K = E_X[\nabla_{\boldsymbol{\theta}} R(X; \boldsymbol{\theta}_0)\nabla_{\boldsymbol{\theta}} R(X; \boldsymbol{\theta}_0)^T]$ in Proposition 3 can not be computed analytically. However, when $n \geq 300$, it can be well approximated by its sample mean $\frac{1}{n}\sum_{i=1}^{n} \nabla_{\boldsymbol{\theta}} R(x_i; \boldsymbol{\theta}_0)\nabla_{\boldsymbol{\theta}} R(x_i; \boldsymbol{\theta}_0)^T$ according to our simulation. From Table 1, we could see that the asymptotical variances computed based on Proposition 3 are close to that computed based on simulation, and the observed coverage appears to be approximately equivalent to the nominal confidence level.

5.2 Multiple pollen tubes

To evaluate and compare the performance of the CMM and CREML procedures, we generated data for each $m = 10$ pollen tubes based on Remark 1 and associated (μ_i, λ_i) simulated from $MVN((\mu, \lambda)^T, \Sigma)$. The true values of parameters used for the simulation were $k_{pf} = 0.1, k_{nf} = 0.1125, \mu = 1, \lambda = 34.1883, \sigma = 4$ and Σ is a diagonal matrix with $\Sigma_{11} = 0.04$ and $\Sigma_{22} = 0.36$. We considered two cases. In case 1, $x = (-5, -1, -0.2, 0.2, 1, 5)$ and $n = 6$. In case 2, x is uniformly sampled from -5 to 5 with step size 0.2 and $n = 51$. Each simulation was done 1000 times. The relative bias, standard deviation and coverage probability for CMM and CREML procedures are shown in Table 3 and Table 4.

From Table 2 and Table 3, we can see that when n is large, CMM procedure and the CREML procedure perform equally well. When n is small, however, the CREML procedure performs better than the CMM procedure. Similar results were also observed by Munther Al-Zaid Yang (2001).

		$\hat{k}_{nf}$	$\hat{k}_{pf}$	$\hat{\mu}$	$\hat{\lambda}$	$\hat{\sigma}_\epsilon$
	Bias	$-3.6 * 10^{-5}$	$4.4 * 10^{-5}$	$-2.8 * 10^{-4}$	$1.0 * 10^{-2}$	$-1.2 * 10^{-2}$
$\sigma = 4$	sd	0.0028	0.0022	0.0138	0.3963	0.1616
	$sd*$	0.0028	0.0023	0.0140	0.4071	
	conv. prob.	0.945	0.956	0.946	0.953	
	Bias	0.0001	0.0002	0.0002	0.0294	-0.0479
$\sigma = 8$	sd	0.0055	0.0046	0.0277	0.8151	0.3274
	sd^*	0.0056	0.0046	0.0279	0.8141	
	conv. prob.	0.95	0.947	0.949	0.944	
	Bias	0.0004	0.0009	0.0008	0.1087	-0.0417
$\sigma = 16$	sd	0.0106	0.0087	0.0527	1.5477	0.6689
	sd^*	0.0111	0.0092	0.0559	1.6283	
	conv. prob.	0.961	0.951	0.958	0.954	

Table 1: CNLS estimators. sd: estimated standard deviation; sd^*: theoretical standard deviation based on proposition 3.

6. POLLEN TUBE DATA ANALYSIS

ROP1 intensities from 12 pollen tubes of Arabidopsis were collected at positions (-10μm, 10 μm) with step size 0.1205 μm.Therefore, $m = 12$ and $n = 173$. The ROP1 intensities in different pollen tubes are believed to have identical distributions. Therefore, quantile normalization was applied to normalize raw data and possible outliers were removed. Notice that the data of $R(x)$ is not 0 even the images show no ROP intensity at x. Therefore, we pool the data sets together and fit the pooled data nonparametrically to obtain $\hat{R}(x)$, and set the background noise to be the smallest value of $\hat{R}(x)$. Then, subtract the background noise from $\hat{R}(x)$ and all the data points. We then standardize $\hat{R}(x)$ and all the data points to $\hat{R}(x)$ with range from 0 to 1 in order to get rid of the unit effects. The values for D, R_{tot} and α used in the study were 0.2, 30 and 1.2, respectively.

We first performed CNLS procedure to the pooled normalized data sets and the individual data sets. The estimates of $k_n f$ and $k_p f$ for individual tubes are presented in table 4 and for pooled data

			$\hat{k}_{nf}$	$\hat{k}_{pf}$	$\hat{\mu}$	$\hat{\lambda}$
Case 1	CMM	Bias	0.0037	0.0021	0.0157	0.0135
		sd	0.0147	0.0068	0.0709	0.4871
		sd^*	0.0139	0.0060	0.0695	0.4569
		conv. prob.	0.932	0.923	0.940	0.942
	CREML	Bias	-0.0004	0.0002	-0.0039	-0.0204
		sd	0.0123	0.0053	0.0614	0.4573
Case 2	CMM	Bias	0.0016	0.0011	0.0061	0.0210
		sd	0.0123	0.0052	0.0607	0.2759
		sd^*	0.0128	0.0053	0.0639	0.2728
		conv. prob.	0.961	0.949	0.960	0.945
	CREML	Bias	0.0015	0.0011	0.0059	0.0181
		sd	0.0122	0.0051	0.0606	0.2737

Table 2: Parameter estimation by CMM and CREML

are 0.1930 and 0.2979, respectively. As we can see, the estimates from each individual tube are close to each other as well as to those obtained from pooled data. This is due to the fact that the sample size within each pollen tube is sufficiently large. Moreover, this indicates that the variation between pollen tubes is not too large. In addition, we performed CMM procedure and CREML procedure to the normalized data sets and the results are shown in table 5.

In Table 5, estimates of all parameters are close between the CMM procedure and the CREML procedure. This is also because the data size is enough ($m = 12, n = 173$). The estimates of k_{nf} and k_{pf} are consistent among the three procedures. The standard deviation of μ and λ are smaller in the CREML procedure than in the CMM procedure, which implies the CREML procedure provides more accuracy. Moreover, there is a large positive correlation among μ and λ, which can be explained by the fact that the positive feedback process and negative feedback process in the first stage of tip growth process has an intrinsic connection since the strength of them both depend on the intensities of active ROP1 on the plasmic membrane.

			$\hat{\sigma}$	$\hat{\Sigma}_{11}$	$\hat{\Sigma}_{22}$
Case 1	CMM	Bias	0.0155	0.0103	0.4409
		sd	0.6050	0.0468	1.9676
	CREML	Bias	-0.0741	-0.0100	0.0974
		sd	0.4147	0.0164	0.6516
Case 2	CMM	Bias	-0.0021	-0.0012	0.0227
		sd	0.1312	0.0183	0.3383
	CREML	Bias	-0.0039	-0.0067	-0.0513
		sd	0.1305	0.0156	0.2942

Table 3: Variance components estimation by CMM and CREML

	$\hat{k}_{nf}$	$\hat{k}_{pf}$		$\hat{k}_{nf}$	$\hat{k}_{pf}$		$\hat{k}_{nf}$	$\hat{k}_{pf}$
Tube 1	0.1866	0.2925	Tube 2	0.2278	0.3337	Tube 4	0.1814	0.2854
Tube 5	0.2205	0.3265	Tube 6	0.1788	0.2748	Tube 7	0.1892	0.2925
Tube 8	0.1917	0.2977	Tube 9	0.2121	0.3188	Tube 10	0.1976	0.3053
Tube 11	0.1939	0.3011	Tube 14	0.1694	0.2766	Tube 15	0.1809	0.2810

Table 4: Results of CNLS procedure for individual tube

6. DISCUSSION

In this paper, we proposed an estimation procedure, CNLS for constrained nonlinear model and two estimation procedures, CMM and CREML for constrained nonlinear mixed model. This was initially motivated from an IDE based parameter estimation problem developed in tip growth process in developmental biology. However, they can also be used in any general constrained modeling problem. All the three procedures perform pretty well when the sample size is sufficiently

	$\hat{k}_{nf}$	$\hat{k}_{pf}$	$\hat{\mu}$	$\hat{\lambda}$	$\hat{\sigma}_{\epsilon}$	$\hat{\sigma}_{\mu}$	$\hat{\sigma}_{\lambda}$	$\hat{\rho}_{\mu,\lambda}$
CMM	0.1942	0.2987	0.9708	0.6477	0.2064	0.0789	0.0393	0.737
CREML	0.1862	0.2873	0.9648	0.6487	0.2267	0.0709	0.0258	0.838

Table 5: Results of CMM and CREML procedure for real data study

large, whereas CREML outperforms CMM when the sample size is small. We used a simple strategy to incorporate the constraints into the objective function before applying simplex method to solve the constrained optimization problem in the estimation procedures, which works quite well.Other optimization methods such as Sequential Quadratic Programming can also be utilized.

The methodology and theoretical result (Proposition 3) for the CNLS estimates are obtained by treating the differential equation parameter estimation problem as the standard nonlinear regression problem which usually has a closed-form objective function. In general, however, differential equation parameter estimation requires numerically solving the differential equation to evaluate the objective function, which produces a higher computational cost and additional numerical error. To deal with the local solution problem, the global optimization problem may need to be considered. Denote $h = max_{1\leq j\leq m-1}|X_{j+1} - X_j|$ as the maximum interval between samples. If there exists a $\gamma > 0$ such that $h = O(n^{-\gamma})$ and the constrained area is bounded with the true parameters μ_0 and λ_0 in the constrained area, then the estimators $\hat{\mu}_n, \hat{\lambda}_n$ will converge to μ_0 and λ_0 almost surely, according to Theorem 3.1 of Xue et al. (2010). This result accounts for the numerical error in solving differential equations.

The proposed CMM procedure is a standard two-stage method, which is not efficient. Although the proposed CREML method is better, the REML method for nonlinear mixed effects models is not easy to converge to the global solution when the parameter space is high. One solution to solve this problem is to use the result of CMM as starting value as we did in the paper.

CONFLICT OF INTERESTS STATEMENT

The authors have declared no conflict of interest.

A. APPENDIX: PROOFS

A.1 Proof of Lemma 1

Based on the classical theory of the differential equation, there are potentially two solutions to the semilinear elliptical equation (3) including the null solution. Therefore, to prove Lemma 1, one only needs to show that there exists a non-null solution σ_0 to equation (3), and $\sigma_0 > 0$ on $[-c, c]$.

The existence of a positive solution to the semilinear elliptic equation $-\partial_x^2 u = f(u)$ is discussed in Lions (1982). In our case, $f(u) = u^\alpha - u$. Therefore, $f(0) = 0$, $f'(0) = -1 < 0$, and $f(u)$ is superlinear since $\frac{f(u)}{u} \to \infty$ as $u \to \infty$. By the Theorem 1.1 in Lions (1982), there exists a positive function σ_0 in $C^2([-c, c])$ that satisfies equation (3). Furthermore, when $c = +\infty$, the existence and uniqueness of solution to the equation (3) can also be proved by the Theorem 1.1.3 in Cazenave and Haraux (1998). From Gidas et al. (1979), it is easy to see that σ_0 is a positive and even function which increases at $[-c, 0]$ and decreases at $[0, c]$.

A.2 Proof of Lemma 2

Similar as the proof of Lemma 1, one only needs to show that there exists a non-null solution $R_{\lambda,\mu}(x)$ to equation (4), and $R_{\lambda,\mu}(x) > 0$ on $[-L_0, L_0]$.

Consider a family of functions $R_{\lambda,\mu}(x) = \lambda\sigma_0(\mu x)$ where $\lambda > 0$, $\mu > 0$, and σ_0 is the unique positive solution to equation (3) for $c = \mu L_0$. Then,

$$\partial_x R_{\lambda,\mu} = \lambda\mu\partial_x\sigma_0(\mu x)$$

$$\partial_x^2 R_{\lambda,\mu} = \lambda\mu^2\partial_x^2\sigma_0(\mu x)$$

By equation (3),

$$-\partial_x^2 R_{\lambda,\mu} = \lambda^{1-\alpha}\mu^2 R_{\lambda,\mu}^\alpha - \mu^2 R_{\lambda,\mu}.$$

Therefore, $R_{\lambda,\mu}$ satisfies $-D\partial_x^2 R_{\lambda,\mu} = -D\mu^2 R_{\lambda,\mu} + D\lambda^{1-\alpha}\mu^2 R_{\lambda,\mu}^\alpha$. Since $\mu, k_{nf}, k_{pf}, D > 0$, we can take $\mu = \sqrt{\frac{k_{nf}}{D}}$ and $\lambda = \left(\frac{k_{pf}}{k_{nf}}\lambda'\right)^{\frac{1}{1-\alpha}}$, then $-D\partial_x^2 R_{\lambda,\mu} = -k_{nf} R_{\lambda,\mu} + \lambda' k_{pf} R_{\lambda,\mu}^\alpha$. Therefore, $R_{\lambda,\mu}$ is the unique positive solution to equation (4).

A.3 Proof of Sufficient Condition

Proof. Since $R_{\lambda'}(x) = R_{\lambda,\mu}(x)$ is a solution to (4), $R_{\lambda'}(x)$ is also a solution to (2) if $\lambda' = \frac{k_{nf}}{k_{pf}}\lambda^{1-\alpha} = \left(1 - \frac{1}{R_{tot}}\|R_{\lambda'}\|_1\right)$, where $\|R_{\lambda'}\|_1 = \int_{-L_0}^{L_0} R_{\lambda,\mu}(x)dx = \lambda\sqrt{\frac{D}{k_{nf}}}\|\sigma_0\|_1$. Denote $g(\lambda) \doteq \frac{k_{nf}}{k_{pf}} - \lambda^{\alpha-1} + \frac{1}{R_{tot}}\lambda^{\alpha}\sqrt{\frac{D}{k_{nf}}}\|\sigma_0\|_1$, then $g'(\lambda) = \lambda^{\alpha-2}\left(-(\alpha-1) + \frac{\alpha}{R_{tot}}\sqrt{\frac{D}{k_{nf}}}\|\sigma_0\|_1\lambda\right)$. The root λ_c of $g'(\lambda)$ is $\lambda_c = \frac{\alpha-1}{\alpha}\sqrt{\frac{k_{nf}}{D}}\frac{R_{tot}}{\|\sigma_0\|_1}$, and $g(\lambda)$ is decreasing in $[0,\lambda_c]$ and increasing in $[\lambda_c,+\infty]$. Notice that $g(0) = \frac{k_{nf}}{k_{pf}}$, $\lim_{+\infty} g = +\infty$, and

$$g(\lambda_c) = \frac{k_{nf}}{k_{pf}} - \frac{1}{\alpha}\left(\frac{\alpha-1}{\alpha}\sqrt{\frac{k_{nf}}{D}}\frac{R_{tot}}{\|\sigma_0\|_1}\right)^{\alpha-1}$$

1. When $g(\lambda_c) > 0$, $g(\lambda) > 0$, no positive solution to (2) can be found from the family of solutions to (4).

2. When $g(\lambda_c) = 0$, $g(\lambda) > 0$ for $\lambda \neq \lambda_c$, therefore one positive solution $R_{\lambda_c,\mu}(x)$ to (2) can be found from the family of solutions to (4).

3. When $g(\lambda_c) < 0$, there exist $\lambda_1 \in [0,\lambda_c]$ and $\lambda_2 \in [\lambda_c,\infty]$ such that $g(\lambda_1) = 0$ and $g(\lambda_2) = 0$, therefore two positive solutions $R_{\lambda_1,\mu}(x)$ and $R_{\lambda_2,\mu}(x)$ to (2) can be found from the family of solutions to (4).

A.4 Proof of Necessary Condition

Proof. It is only necessary to show that for any positive solution R of (2) on $[-L_0, L_0]$, there exist $\lambda,\mu > 0$ such that $\sigma_0(x) = \frac{1}{\lambda}R(\frac{x}{\mu})$ is a solution to (3) on $\left[-\frac{L_0}{\mu},\frac{L_0}{\mu}\right]$. Denote $\bar{\lambda} = \frac{1}{\lambda}$, $\bar{\mu} = \frac{1}{\mu}$, then $\frac{\partial\sigma_0(x)}{\partial x} = \bar{\lambda}\bar{\mu}\frac{\partial R(\bar{\mu}x)}{\partial(\bar{\mu}x)}$ and $\frac{\partial^2\sigma_0(x)}{\partial x^2} = \bar{\lambda}\bar{\mu}^2\frac{\partial^2 R(\bar{\mu}x)}{\partial(\bar{\mu}x)^2}$. $\sigma_0(x)$ is a solution to (3) on $[-L_0\bar{\mu}, L_0\bar{\mu}]$ if and only if

$$\begin{aligned}
&-\frac{\partial^2\sigma_0(x)}{\partial x^2} = -\sigma_0(x) + \sigma_0^{\alpha}(x) \\
&-\bar{\lambda}\bar{\mu}^2 R''(\bar{\mu}x) = -\bar{\lambda}R(\bar{\mu}x) + \bar{\lambda}^{\alpha}R^{\alpha}(\bar{\mu}x) \\
&-\bar{\mu}^2\frac{k_{nf}R(\bar{\mu}x)}{D} + \bar{\mu}^2\frac{k_{pf}R^{\alpha}(\bar{\mu}x)}{D}\left(1 - \frac{\int_{-L_0}^{L_0} R(x)dx}{R_{tot}}\right) = -R(\bar{\mu}x) + \bar{\lambda}^{\alpha-1}R^{\alpha}(\bar{\mu}x)
\end{aligned}$$

when $\bar{\mu} = \sqrt{\frac{D}{k_{nf}}}$, $\bar{\lambda}$ can be obtained by solving the equality

$$\frac{k_{pf}}{k_{nf}}R^{\alpha}(\bar{\mu}x)\left(1 - \frac{\int_{-L_0}^{L_0} R(x)dx}{R_{tot}}\right) = \bar{\lambda}^{\alpha-1}R^{\alpha}(\bar{\mu}x)$$

for which $\bar{\lambda} = \left[\frac{k_{pf}}{k_{nf}}\left(1 - \frac{\int_{-L_0}^{L_0} R(x)dx}{R_{tot}}\right)\right]^{\frac{1}{\alpha-1}}$. Hence, $\bar{\lambda}$ exists if and only if $\frac{\int_{-L_0}^{L_0} R(x)dx}{R_{tot}} < 1$. Suppose $\frac{\int_{-L_0}^{L_0} R(x)dx}{R_{tot}} \geq 1$, then the right hand side of equation (2) is nonpositive and therefore the left hand side of equation (2) must be nonpositive. That is, $R''(x) > 0$. Therefore, $R(x)$ must be a convex function. This is impossible because $R(x)$ is a positive function with $R(-L_0) = R(L_0) = 0$. Therefore, $\frac{\int_{-L_0}^{L_0} R(x)dx}{R_{tot}} < 1$ always holds for $R(x) > 0$ and $\bar{\lambda}$ exists, which completes the proof.

A.5 Proof of Remark 2

By Lemma 1, σ_0 is a positive and even function which increases at $[-c, 0]$ and decreases at $[0, c]$. Therefore, $R_{\lambda,\mu}(x) = \lambda\sigma_0(\mu x)$ preserves the same properties. Moreover, in the proof of Lemma 1, the function $f(x) = x^\alpha - x$ is such that $f(1) = 0$, and $f(x) > 0$ for $x > 1$. Therefore, by Theorem 3.1 of Lions (1982), $\max_x \sigma_0(x) > 1$. As a result, $\max_x R_{\lambda,\mu}(x) = \lambda \times \max_x \sigma_0(\mu x) > \lambda$.

A.6 Proof of Proposition 1

Lemma 3. *for any $\mu > 0$ and $\lambda > 0$, the function $h(\mu, \lambda) = \lambda^{\alpha-1} - \lambda^\alpha \frac{\|\sigma_0\|_1}{\mu R_{tot}} - \frac{1}{\alpha}\left(\frac{\alpha-1}{\alpha}\frac{\mu R_{tot}}{\|\sigma_0\|_1}\right)^{\alpha-1}$ is always non-positive.*

Proof. For any fixed $\mu > 0$, h is a function of λ whose first-order derivative is 0 if and only if $\lambda \doteq \lambda_c = \frac{\alpha-1}{\alpha}\frac{\mu R_{tot}}{\|\sigma_0\|_1}$. Then, we have

$$h(\lambda_c) = \lambda_c^{\alpha-1} - \lambda_c^\alpha \frac{\|\sigma_0\|_1}{\mu R_{tot}} - \frac{1}{\alpha}\left(\frac{\alpha-1}{\alpha}\frac{\mu R_{tot}}{\|\sigma_0\|_1}\right)^{\alpha-1} = 0$$

$$h(0) = -\frac{1}{\alpha}\left(\frac{\alpha-1}{\alpha}\frac{\mu R_{tot}}{\|\sigma_0\|_1}\right)^{\alpha-1} < 0$$

$$h(+\infty) = -\infty < 0$$

Notice that $h(\lambda)$ is a continuous function of λ, we can conclude that $h(\lambda) \leq 0$ based on the above three equations. Therefore, Lemma 3 holds.

When the constraints in model (7) are satisfied, $g(\lambda)$ has at least one solution. As a result, $\frac{k_{nf}}{k_{pf}} = \lambda^{\alpha-1} - \frac{1}{R_{tot}}\lambda^\alpha \frac{1}{\mu}\|\sigma_0\|_1 > 0$ and $\mu > 0$ and $\lambda > 0$. Therefore, the constraints in model (8) hold. When the constraints in model (8) are satisfied, we can convert μ and λ to k_{nf} and k_{pf} by solving $k_{nf} = D\mu^2$ and $\frac{k_{nf}}{k_{pf}} = \lambda^{\alpha-1} - \frac{1}{R_{tot}}\lambda^\alpha \frac{1}{\mu}\|\sigma_0\|_1$. The solution of k_{nf} and k_{pf} is such that $k_{nf} > 0$, $k_{pf} > 0$ and by Lemma 3, $\Lambda(k_{nf}, k_{pf}, D, R_{tot}, \sigma_0) = \frac{k_{nf}}{k_{pf}} - \frac{1}{\alpha}(\frac{\alpha-1}{\alpha}\sqrt{\frac{k_{nf}}{D}}\frac{R_{tot}}{\|\sigma_0\|_1})^{\alpha-1} = \lambda^{\alpha-1} - \lambda^\alpha \frac{\|\sigma_0\|_1}{R_{tot}\mu} - \frac{1}{\alpha}\left(\frac{\alpha-1}{\alpha}\frac{R_{tot}\mu}{\|\sigma_0\|_1}\right)^{\alpha-1} \leq 0$. Therefore, the constraints in model (7) hold.

A.7 Proof of Proposition 2

Lemma 4. *Let $A = (a_{ij})_{2\times 2}$ denote a symmetric two by two matrix. Suppose all the four elements of A are bounded in $[-B, B]$ for some $B > 0$, then $A \le 2BI_2$.*

Proof. For any vector $\boldsymbol{x} = (x_1, x_2)^T$, $\boldsymbol{x}^T A\boldsymbol{x} = a_{11}x_1^2 + 2a_{12}x_1x_2 + a_{22}x_2^2 \le 2Bx_1^2 + 2Bx_2^2 = 2B\boldsymbol{x}^T\boldsymbol{x}$. Therefore, $A \le 2BI_2$ and Lemma 4 holds.

Denote $z = (z_\mu, z_\lambda)^T = n^{1/2}(\boldsymbol{\theta} - \boldsymbol{\theta_0})$. It can be easily seen that minimizing (10) under the constraint (9) is equivalent to

$$\begin{aligned} &\min_z \textstyle\sum_{j=1}^n \{[\epsilon_j + R(x_j, \boldsymbol{\theta_0}) - R(x_j, \boldsymbol{\theta_0} + n^{-1/2}z)]^2 - \epsilon_j^2\} \\ \texttt{s.t.}\, &g_1(\boldsymbol{\theta_0} + n^{-1/2}z) = -(\mu_0 + n^{-1/2}z_\mu)R_{tot} + (\lambda_0 + n^{-1/2}z_\lambda) \parallel \boldsymbol{\sigma_0} \parallel_1 < 0 \\ &g_2(\boldsymbol{\theta_0} + n^{-1/2}z) = -(\mu_0 + n^{-1/2}z_\mu) < 0 \\ &g_3(\boldsymbol{\theta_0} + n^{-1/2}z) = -(\lambda_0 + n^{-1/2}z_\lambda) < 0 \end{aligned} \tag{A.1}$$

where ϵ_j are i.i.d with $N(0, \sigma^2)$.

Assume the optimal solution of (A.1) exists and denote it by $\hat{z}_n$. Then $\hat{z}_n = n^{1/2}(\hat{\boldsymbol{\theta}}_n - \boldsymbol{\theta}_0)$. Therefore to prove proposition 2, we only need to prove $\hat{z}_n \xrightarrow{d} N(0, \sigma^2K^{-1})$, which can be achieved in the following two steps. First, we prove when $n \to \infty$ the limit problem of problem (A.1) is

$$\texttt{min}\ z'Kz - 2z'\xi \tag{A.2}$$

where $\xi \sim N(0, \sigma_\epsilon^2 K)$. Then, we prove the solution to problem (A.1) converges in distribution to the solution to problem (A.2).

Step 1: Limit problem of (A.1)

Denote the objective function $F_n(\epsilon, z) = \sum_{j=1}^n \{[\epsilon_j + R(x_j, \boldsymbol{\theta_0}) - R(x_j, \boldsymbol{\theta_0} + n^{-1/2}z)]^2 - \epsilon_j^2\}$ and parameter space $S_n = \{z : g_1(\boldsymbol{\theta_0} + n^{-1/2}z) < 0, g_2(\boldsymbol{\theta_0} + n^{-1/2}z) < 0, g_3(\boldsymbol{\theta_0} + n^{-1/2}z) < 0\}$. To formulate the limit problem of (A.1), we have the following results.

Result 1: When $\sigma^2 = 1$, for each fixed $z \in \mathbb{R}^2$, $F_n(\epsilon, z)$ converges in distribution to $F(\xi, z) = z'Kz - 2z'\xi$, where $\xi \sim N(0, K)$.

(i) As specified in Section 4, $\epsilon_1, \epsilon_2, \ldots, \epsilon_n$ are *i.i.d.* with $E(\epsilon_i) = 0$ and $Var(\epsilon_i) = \sigma^2 = 1$.

(ii) $R(x_j; \boldsymbol{\theta}) = \lambda\sigma_0(\mu x_j)$, $j = 1, \ldots, n$, are differentiable in $\boldsymbol{\theta}$ since $\sigma_0(\mu x_j)$ is differentiable in

μ. By Taylor expansion,

$$R(x_j;\boldsymbol{\theta}) = R(x_j;\boldsymbol{\theta}_0) + \nabla_{\boldsymbol{\theta}} R(x_j;\boldsymbol{\theta}_0)^T(\boldsymbol{\theta}-\boldsymbol{\theta}_0) + \frac{1}{2}(\boldsymbol{\theta}-\boldsymbol{\theta}_0)^T \Delta_{\boldsymbol{\theta}} R(x_j;\boldsymbol{\theta}_0)(\boldsymbol{\theta}-\boldsymbol{\theta}_0) + o(\|\boldsymbol{\theta}-\boldsymbol{\theta}_0\|^2)$$

where $\bigtriangledown_{\boldsymbol{\theta}} R(x_j;\boldsymbol{\theta_0}) = \begin{pmatrix} \lambda_0 x_j \sigma_0'(\mu_0 x_j) \\ \sigma_0(\mu_0 x_j) \end{pmatrix}$ and $\triangle_{\boldsymbol{\theta}} R(x_j;\boldsymbol{\theta_0}) = \begin{pmatrix} \lambda_0 x_j^2 \sigma_0''(\mu_0 x_j) & x_j \sigma_0'(\mu_0 x_j) \\ x_j \sigma_0'(\mu_0 x_j) & 0 \end{pmatrix}$.

Let $r_j(\boldsymbol{\theta}) = \{R(x_j;\boldsymbol{\theta}) - R(x_j;\boldsymbol{\theta_0}) - \bigtriangledown_{\boldsymbol{\theta}} R(x_j;\boldsymbol{\theta_0})^T(\boldsymbol{\theta}-\boldsymbol{\theta_0})\}/ \parallel \boldsymbol{\theta}-\boldsymbol{\theta_0} \parallel^2$. Since $R(x_j;\boldsymbol{\theta})$, $\bigtriangledown_{\boldsymbol{\theta}} R(x_j;\boldsymbol{\theta_0})^T(\boldsymbol{\theta}-\boldsymbol{\theta_0})$,$\parallel \boldsymbol{\theta}-\boldsymbol{\theta_0} \parallel^2$ are continuous on $\boldsymbol{\theta}$, $r_j(\boldsymbol{\theta})$ is a continuous function on $\boldsymbol{\theta}$.

It's obvious that there exists $B > 0$ such that all elements in $\triangle_{\boldsymbol{\theta}} R(x_j, \boldsymbol{\theta_0})$ are bounded by $[-B, B]$. Therefore, from Lemma 4, we have

$$\begin{aligned} |r_j(\boldsymbol{\theta})| \parallel \boldsymbol{\theta}-\boldsymbol{\theta}_0 \parallel^2 &= |\frac{1}{2}(\boldsymbol{\theta}-\boldsymbol{\theta}_0)^T \Delta_{\boldsymbol{\theta}} R(x_j;\boldsymbol{\theta}_0)(\boldsymbol{\theta}-\boldsymbol{\theta}_0) + o(\|\boldsymbol{\theta}-\boldsymbol{\theta}_0\|^2)| \\ &\leq \frac{1}{2}(\boldsymbol{\theta}-\boldsymbol{\theta}_0)^T 2BI_2(\boldsymbol{\theta}-\boldsymbol{\theta}_0) \\ &= B\|\boldsymbol{\theta}-\boldsymbol{\theta}_0\|^2 \end{aligned}$$

Therefore, $|r_j(\boldsymbol{\theta})| \leq B$ and $\lim_{n\to\infty} \frac{1}{n}\sum_{j=1}^n r_j^2(\boldsymbol{\theta}) \leq B^2 < \infty$ holds in the whole parameter space.

(iii) Since $\bigtriangledown_{\boldsymbol{\theta}} R(x_j, \boldsymbol{\theta}_0) \bigtriangledown_{\boldsymbol{\theta}} R(x_j, \boldsymbol{\theta}_0)' = \begin{pmatrix} \lambda_0^2 x_j^2 \sigma_0'(\mu_0 x_j)^2 & \lambda_0 x_j \sigma_0(\mu_0 x_j)\sigma_0'(\mu_0 x_j) \\ \lambda_0 x_j \sigma_0(\mu_0 x_j)\sigma_0'(\mu_0 x_j) & \sigma_0(\mu_0 x_j)^2 \end{pmatrix}$, all the elements in $\bigtriangledown_{\boldsymbol{\theta}} R(x_j, \boldsymbol{\theta}_0) \bigtriangledown_{\boldsymbol{\theta}} R(x_j, \boldsymbol{\theta}_0)'$ are bounded. By Kolmogorov's Strong Law of Large Numbers (SLLN), we have

$$\frac{1}{n}\sum_{j=1}^n \bigtriangledown_{\boldsymbol{\theta}} R(x_j, \boldsymbol{\theta}_0) \bigtriangledown_{\boldsymbol{\theta}} R(x_j, \boldsymbol{\theta}_0)' \xrightarrow{a.s.} K$$

where

$$K = \begin{pmatrix} E_X[\lambda_0^2 X^2 \sigma_0'(\mu_0 X)^2] & E_X[\lambda_0 X \sigma_0(\mu_0 X)\sigma_0'(\mu_0 X)] \\ E_X[\lambda_0 X \sigma_0(\mu_0 X)\sigma_0'(\mu_0 X)] & E_X[\sigma_0(\mu_0 X)^2] \end{pmatrix}$$

By Cauchy-Schwarz inequality we have

$$det(K) = E_X[\lambda_0^2 X^2 \sigma_0'(\mu_0 X)^2] E_X[\sigma_0(\mu_0 X)^2] - (E_X[\lambda_0 X \sigma_0(\mu_0 X)\sigma_0'(\mu_0 X)])^2 \geq 0$$

However, if equality holds, it implies that $\lambda_0 X \sigma_0'(\mu_0 X)$ and $\sigma_0(\mu_0 X)$ are linearly dependent, i.e., there exists a non-zero scalar $a \in R$ such that $\lambda_0 X \sigma_0'(\mu_0 X) = a\sigma_0(\mu_0 X)$ holds everywhere since $\sigma_0(\mu_0 X)$ and $\sigma_0'(\mu_0 X)$ are both continuously differentiable. As a result, $\sigma_0(\mu_0 X)$ is a solution to the linear ODE $\lambda_0 u'(X) - au(X) = 0$. However, the solution is $u(X) = Ce^{\frac{a}{\lambda_0}x}$ which can not satisfy the boundary condition required for $\sigma_0(X)$. Therefore $det(K) > 0$. Since $trace(K) > 0$, both eigenvalues of K are positive. So K is positive definite.

Therefore, $\lim_{n\to\infty} \dfrac{1}{n} \sum_{j=1}^{n} \bigtriangledown_{\boldsymbol{\theta}} R(x_j, \boldsymbol{\theta}_0) \bigtriangledown_{\boldsymbol{\theta}} R(x_j, \boldsymbol{\theta}_0)' = K$ exists and is positive definite.

From Theorem 1 of Wang (1996), we have $F_n(\epsilon, z)$ converges in distribution to $F(\xi, z) = z'Kz - 2z'\xi$.

Result 2: It is obvious that $g_i(\boldsymbol{\theta})$ are continuously differentiable and there exists no equality constraints. Also because

$$\begin{cases} g_1(\boldsymbol{\theta}_0) = \mu_0 R_{tot} - \lambda_0 \parallel \sigma_0 \parallel_1 \neq 0 \\ g_2(\boldsymbol{\theta}_0) = \mu_0 \neq 0 \\ g_3(\boldsymbol{\theta}_0) = \lambda_0 \neq 0 \end{cases}.$$

I is an empty set. Therefore, by theorem 2 of Wang (1996), we have parameter space S_n converges in Kuratowski's sense to S which is the parameter space of A.2. Combining part 1 and part 2, the limit problem of (A.1) is minimizing $z'Kz - 2z'\xi$ without constraint.

Step 2 Convergence of solution to (A.1)

According to theorem 3-6 of Wang (1996), the solution to limit problem A.2 should be unique at $B(M) = z :\parallel z \parallel < M$ for any large M, so that the solution to (A.1) converges in distribution to the solution to (A.2),

Since limit problem (A.2) is minimizing $z'Kz - 2z'\xi$ without constraint, there is a unique solution $z = K^{-1}\xi$ at $B(M) = z :\parallel z \parallel < M$ for any $M > \parallel K^{-1}\xi \parallel$. Therefore, by theorem 3-6 of Wang (1996), $\hat{z}_n$ of problem (A.1) converges in distribution to $z = K^{-1}\xi \sim N(0, \sigma^2 K^{-1})$, i.e. $\hat{z}_n = \sqrt{n}(\hat{\theta}_n - \theta_0) \xrightarrow{d} N(0, \sigma^2 K^{-1})$. This completes the proof.

For any $\sigma^2 > 0$, based on Theorem 4 and 5 of Jennrich Jennrich (1969),

$$n^{-\frac{1}{2}} \sum_{i=1}^{n} \nabla_{\boldsymbol{\theta}} R(X_i; \boldsymbol{\theta}_0) \boldsymbol{\epsilon}_i \xrightarrow{d} N(0, \sigma^2 K)$$

As a result, $F_n(\boldsymbol{\epsilon}_i, \boldsymbol{z})$ will converge in distribution to $\boldsymbol{z}'K\boldsymbol{z} - 2\boldsymbol{z}'\boldsymbol{\xi}$ where $\boldsymbol{\xi}$ is a random vector following $N(0, \sigma^2 K)$. In fact, based on Theorem 1-5 of Jennrich Jennrich (1969), Theorem 1-6 of Wang (1996) still hold even if σ^2 is unknown.

A.8 Proof of Proposition 3

In this section, we want to prove the consistency of $\hat{\sigma}_n^2 = \frac{1}{n}\sum_{j=1}^n (y_j - R(x_j, \hat{\boldsymbol{\theta}}_n))^2$, i.e. $\hat{\sigma}_n^2 \xrightarrow{p} \sigma^2$.

$$\begin{aligned}\hat{\sigma}_n^2 &= \frac{1}{n}\sum_{j=1}^n (y_j - R(x_j, \hat{\boldsymbol{\theta}}_n))^2 = \frac{1}{n}\sum_{j=1}^n (R(x_j, \boldsymbol{\theta}_0) + \epsilon_j - R(x_j, \hat{\boldsymbol{\theta}}_n))^2 \\ &= \frac{1}{n}\sum_{j=1}^n (R(x_j, \boldsymbol{\theta}_0) - R(x_j, \hat{\boldsymbol{\theta}}_n))^2 + \frac{2}{n}\sum_{j=1}^n (R(x_j, \boldsymbol{\theta}_0) - R(x_j, \hat{\boldsymbol{\theta}}_n))\epsilon_j + \frac{1}{n}\sum_{j=1}^n \epsilon_j^2\end{aligned} \tag{A.3}$$

First, we prove that $\frac{1}{n}\sum_{j=1}^n (R(x_j, \boldsymbol{\theta}_0) - R(x_j, \hat{\boldsymbol{\theta}}_n))^2 \xrightarrow{p} 0$. From proof of Proposition 2, we have $\frac{1}{n}\sum_{j=1}^n \bigtriangledown_{\boldsymbol{\theta}} R(x_j, \boldsymbol{\theta}_0) \bigtriangledown_{\boldsymbol{\theta}} R(x_j, \boldsymbol{\theta}_0)^T \xrightarrow{a.s.} K$ and $K \leq 2BI$. Since $\sqrt{n}(\hat{\boldsymbol{\theta}}_n - \boldsymbol{\theta}_0) \xrightarrow{d} N(0, \sigma^2 K^{-1})$, we have $\hat{\boldsymbol{\theta}}_n \xrightarrow{L_2} \boldsymbol{\theta}_0$. Therefore, we have

$$\begin{aligned}&\frac{1}{n}\sum_{j=1}^n (R(x_j, \boldsymbol{\theta}_0) - R(x_j, \hat{\boldsymbol{\theta}}_n))^2 \\ &= (\hat{\boldsymbol{\theta}}_n - \boldsymbol{\theta}_0)^T [\frac{1}{n}\sum_{j=1}^n \bigtriangledown_{\boldsymbol{\theta}} R(x_j, \boldsymbol{\theta}_0) \bigtriangledown_{\boldsymbol{\theta}} R(x_j, \boldsymbol{\theta}_0)^T](\hat{\boldsymbol{\theta}}_n - \boldsymbol{\theta}_0) + o(\parallel \hat{\boldsymbol{\theta}}_n - \boldsymbol{\theta} \parallel^2) \\ &\xrightarrow{p} 0\end{aligned} \tag{A.4}$$

Since $\bigtriangledown_{\boldsymbol{\theta}} R(x_j, \boldsymbol{\theta}_0) = \begin{pmatrix} \lambda_0 x_j \sigma_0'(\mu_0 x_j) \\ \sigma_0(\mu_0 x_j) \end{pmatrix}$ which is continuous and bounded, by theorem 4 of Jennrich (1969), we have $\frac{1}{n}\sum_{j=1}^n \bigtriangledown_{\boldsymbol{\theta}} R(x_j, \boldsymbol{\theta}_0)\epsilon_j \xrightarrow{p} 0$. Therefore, we have

$$\frac{1}{n}\sum_{j=1}^n (R(x_j, \boldsymbol{\theta}_0) - R(x_j, \hat{\boldsymbol{\theta}}_n))\epsilon_j = (\hat{\boldsymbol{\theta}}_n - \boldsymbol{\theta}_0)^T \{\frac{1}{n}\sum_{j=1}^n \bigtriangledown_{\boldsymbol{\theta}} R(x_j, \boldsymbol{\theta}_0)\epsilon_j\} + o(\parallel \hat{\boldsymbol{\theta}}_n - \boldsymbol{\theta}_0 \parallel) \xrightarrow{p} 0 \tag{A.5}$$

By SLLN, $\frac{1}{n}\sum_{j=1}^n \epsilon_j^2 \xrightarrow{a.s.} \sigma^2$. From equation (A.3), (A.4) and (A.5), we have $\hat{\sigma}_n^2 \xrightarrow{p} \sigma^2$.

A.9 Proof of Proposition 4

Since $\hat{\boldsymbol{\theta}}_i = (\hat{\mu}_i, \hat{\lambda}_i)^T$ is obtained by CNLS for each single pollen tube, from Proposition 3 we have

$$\sqrt{n}(\hat{\boldsymbol{\theta}}_i - \boldsymbol{\theta}_i) \xrightarrow{d} MVN\left(\mathbf{0}, \sigma^2 (K_i)^{-1}\right)$$

for each given $\boldsymbol{\theta}_i$, where $K_i = E_X[\nabla_{\boldsymbol{\theta}_i} R(X;\boldsymbol{\theta}_i)\nabla_{\boldsymbol{\theta}_i} R(X;\boldsymbol{\theta}_i)^T]$. Since $\boldsymbol{\theta}_i \sim MVN(\boldsymbol{\theta},\Sigma)$, the unconditional asymptotic mean and variance of $\hat{\boldsymbol{\theta}}_i$ are

$$\begin{aligned}
E(\hat{\boldsymbol{\theta}}_i) &= E_{\boldsymbol{\theta}}[E_\epsilon(\hat{\boldsymbol{\theta}}_i|\boldsymbol{\theta}_i)] \to E_{\boldsymbol{\theta}}(\boldsymbol{\theta}_i) = \boldsymbol{\theta} \\
Var(\hat{\boldsymbol{\theta}}_i) &= Var_{\boldsymbol{\theta}}[E_\epsilon(\hat{\boldsymbol{\theta}}_i|\boldsymbol{\theta}_i)] + E_{\boldsymbol{\theta}}[Var_\epsilon(\hat{\boldsymbol{\theta}}_i|\boldsymbol{\theta}_i)] \to Var_{\boldsymbol{\theta}}[\boldsymbol{\theta}_i] + E_{\boldsymbol{\theta}}[(nK_i)^{-1}\sigma^2] \\
&= \Sigma + \sigma^2 E_{\boldsymbol{\theta}}[(nK_i)^{-1}] \doteq \tilde{\Sigma}
\end{aligned}$$

Therefore, $\{\hat{\boldsymbol{\theta}}_i : i = 1,\cdots,m\}$ are *i.i.d.* with common asymptotic mean and variance. Since $\hat{\boldsymbol{\theta}} = m^{-1}\sum \hat{\boldsymbol{\theta}}_i$, from SLLN and CLT, we have

$$\begin{aligned}
\frac{1}{m-1}\sum_{i=1}^{m}(\hat{\boldsymbol{\theta}}_i - \hat{\boldsymbol{\theta}})(\hat{\boldsymbol{\theta}}_i - \hat{\boldsymbol{\theta}})^T &\xrightarrow{p} \tilde{\Sigma} \\
\hat{\boldsymbol{\theta}} &\xrightarrow{p} \boldsymbol{\theta} \\
\sqrt{m}\tilde{\Sigma}^{-\frac{1}{2}}(\hat{\boldsymbol{\theta}} - \boldsymbol{\theta}) &\xrightarrow{d} \boldsymbol{Z}
\end{aligned}$$

with $\boldsymbol{Z} \sim N(0, I_2)$.

Furthermore, we have

$$\begin{aligned}
&E(T_i^{-1}) = E_{\boldsymbol{\theta}}[E_\epsilon(T_i^{-1}|\boldsymbol{\theta}_i)] = E_{\boldsymbol{\theta}}[E_\epsilon(\left(\left[\frac{\partial \boldsymbol{R}_i}{\partial \boldsymbol{\theta}_i^T}\right]^T \left[\frac{\partial \boldsymbol{R}_i}{\partial \boldsymbol{\theta}_i^T}\right]|_{\boldsymbol{\theta}_i=\hat{\boldsymbol{\theta}}_i}\right)^{-1} |\boldsymbol{\theta}_i)] \\
&\xrightarrow{p} E_{\boldsymbol{\theta}}\left[\left(\left[\frac{\partial \boldsymbol{R}_i}{\partial \boldsymbol{\theta}_i^T}\right]^T \left[\frac{\partial \boldsymbol{R}_i}{\partial \boldsymbol{\theta}_i^T}\right]\right)^{-1}\right] = E_{\boldsymbol{\theta}}\left[\left(\sum_{j=1}^{n}\left[\frac{\partial R(X_{ij};\boldsymbol{\theta}_i)}{\partial \boldsymbol{\theta}_i^T}\right]\left[\frac{\partial R(X_{ij};\boldsymbol{\theta}_i)}{\partial \boldsymbol{\theta}_i^T}\right]^T\right)^{-1}\right] \\
&\xrightarrow{p} E_{\boldsymbol{\theta}}[\big(nE_X[\nabla_{\boldsymbol{\theta}_i} R(X;\boldsymbol{\theta}_i)\nabla_{\boldsymbol{\theta}_i} R(X;\boldsymbol{\theta}_i)^T]\big)^{-1}] = E_{\boldsymbol{\theta}}[(nK_i)^{-1}]
\end{aligned}$$

The first "$\xrightarrow{p}$" in the above equation holds since $\hat{\boldsymbol{\theta}}_i \xrightarrow{p} \boldsymbol{\theta}_i$. The second "$\xrightarrow{p}$" holds by SLLN of X. Therefore, $\{T_i^{-1} : i = 1,\cdots,m\}$ are *i.i.d.* with the same asymptotic mean, and so by SLLN we have that $\frac{1}{m}\sum_{i=1}^m T_i^{-1} \xrightarrow{p} E_{\boldsymbol{\theta}}[(nK_i)^{-1}]$. In addition, it's assumed that $\hat{\sigma}^2 \xrightarrow{p} \sigma^2$. Therefore, by *Slutsky's* Theorem, $\hat{\Sigma} \xrightarrow{p} \tilde{\Sigma} - \sigma^2 E_{\boldsymbol{\theta}}[(nK_i)^{-1}] = \Sigma$.

Based on the asymptotical result of $\hat{\Sigma}$, we know that $\hat{\tilde{\Sigma}} = \hat{\Sigma} + \hat{\sigma}^2 E_{\boldsymbol{\theta}}[(nK_i)^{-1}] \xrightarrow{p} \tilde{\Sigma}$. We also have proved that $\hat{\boldsymbol{\theta}}$, $\sqrt{m}(\hat{\boldsymbol{\theta}} - \boldsymbol{\theta}) \xrightarrow{d} \tilde{\Sigma}^{\frac{1}{2}}\boldsymbol{Z}$. Therefore, by *Slutsky's* Theorem we have $\sqrt{m}\hat{\tilde{\Sigma}}^{-\frac{1}{2}}(\hat{\boldsymbol{\theta}} - \boldsymbol{\theta}) \xrightarrow{d} \boldsymbol{Z}$. This completes the proof of Proposition 4.

REFERENCES

Altschuler, S. J., Angenent, S. B., Wang, Y., and Wu, L. (2008). On the spontaneous emergence of cell polarity. *Nature* **454,** 886–889.

Bader, G. and Ascher, U. (1987). A new basis implementation for a mixed order boundary value ode solver. *SIAM Journal on Scientific and Statistical Computing* **8,** 483–500.

Berken, A., Thomas, C., and Wittinghofer, A. (2005). A new family of rhogefs activates the rop molecular switch in plants. *Nature* **436,** 1176–1180.

Brunel, N. (2008). Parameter estimation of ODE's via nonparametric estimators. *Electronic journal of Statistics* .

Brunel, N., Clairon, Q., and Dlche, F. (2014). Parametric Estimation of Ordinary Differential Equations with Orthogonality Conditions. *Journal of the American Statistical Association* **109,** 173–185.

Campas, O. and Mahadevan, L. (2009). Shape and Dynamics of Tip-Growing Cells. *Current Biology* **19,** 2102–2107.

Cash, J. and Mazzia, F. (2005). A new mesh selection algorithm, based on conditioning, for two-point boundary value codes. *Journal of Computational and Applied Mathematics* **184,** 362 – 381.

Cazenave, T. and Haraux, A. (1998). *An introduction to semilinear evolution equations*, volume 13 of *Oxford Lecture Series in Mathematics and its Applications.* The Clarendon Press Oxford University Press, New York.

Dumais, J., Shaw, S., Steele, C., Long, S., and Ray, P. (2006). An anisotropic-viscoplastic model of plant cell morphogenesis by tip growth. *The International Journal of Developmental Biology* **50,** 209–222.

Fayant, P., Girlanda, O., Chebli, Y., Aubin, C., Villemure, I., and Geitmann, A. (2010). Finite element model of polar growth in pollen tubes. *The Plant Cell* **22,** 2579–2593.

Gidas, B., Ni, W., and Nirenberg, L. (1979). Symmetry and related properties via the maximum principle. *Communications in Mathematical Physics* **68,** 209–243.

Gu, Y., Fu, Y., Dowd, P., Li, S., Vernoud, V., Gilroy, S., and Yang, Z. (2005). A rho family gtpase controls actin dynamics and tip growth via two counteracting downstream pathways in pollen tubes. *The Journal of Cell Biology* **169,** 127–138.

Guedj, J., Thiebaut, R., and Commenges, D. (2007). Maximum likelihood estimation in dynamical models of hiv. *Biometrics* **63,** 1198–1206.

Hepler, P., Vidali, L., and Cheung, A. (2001). Polarized cell growth in higher plants. *Annual Review of Cell and Developmental Biology* **17,** 159–187.

Huang, Y. and Wu, H. (2006a). A bayesian approach for estimating antiviral efficacy in hiv dynamic models. *Journal of Applied Statistics* **33,** 155–174.

Huang, Y. and Wu, H. (2006b). A bayesian approach for estimating antiviral efficacy in hiv dynamic models. *Journal of Applied Statistics* **33,** 155–174.

Hwang, J., Vernoud, V., Szumlanski, A., Nielsen, E., and Yang, Z. (2008). A tip-localized rhogap controls cell polarity by globally inhibiting rho gtpase at the cell apex. *Current Biology* **18,** 1907–1916.

Hwang, J., Wu, G., Yan, A., Lee, Y., Grierson, C., and Yang, Z. (2010). Pollen-tube tip growth requires a balance of lateral propagation and global inhibition of rho-family gtpase activity. *Journal of Cell Science* **123,** 340–350.

J. H. Kroeger, A Geitmann, M. G. (2008). Model for calcium dependent oscillatory growth in pollen tubes. . *Journal of Theoretical Biology* **253,** 363–374.

Jennrich, R. I. (1969). Asymptotic Properties of Non-Linear Least Squares Estimators. *The Annals of Mathematical Statistics* **40,** 633–643.

Ke, C. and Wang, Y. (2001). Semiparametric nonlinear mixed-effects models and their applications. *Journal of the American Statistical Association* **96,** 1272–1298.

Kost, B., Lemichez, E., Spielhofer, P., Hong, Y., Tolias, K., Carpenter, C., and Chua, N. (1999). Rac homologues and compartmentalized phosphatidylinositol 4, 5-bisphosphate act in a common pathway to regulate polar pollen tube growth. *The Journal of Cell Biology* **145,** 317–330.

Lee, Y., Szumlanski, A., Nielsen, E., and Yang, Z. (2008). Rho-gtpase-dependent filamentous actin dynamics coordinate vesicle targeting and exocytosis during tip growth. *The Journal of Cell Biology* **181,** 1155–1168.

Lee, Y. and Yang, Z. (2008). Tip growth: Signaling in the apical dome. *Current Opinion in Plant Biology* **11,** 662–671.

Li, H., Lin, Y., Heath, R., Zhu, M., and Yang, Z. (1999). Control of pollen tube tip growth by a rop gtpase-dependent pathway that leads to tip-localized calcium influx. *Plant Cell* **11,** 1731–1742.

Li, H., Wu, G., Ware, D., Davis, K., and Yang, Z. (1998). Arabidopsis rho-related gtpases: differential gene expression in pollen and polar localization in fission yeast. *Plant Physiology* **118,** 407–417.

Li, L., Brown, M., Lee, K., and Gupta, S. (2002). Estimation and inference for a spline-enhanced population pharmacokinetic model. *Biometrics* **58,** 601–611.

Lin, Y., Wang, Y., Zhu, J., and Yang, Z. (1996). Localization of a rho gtpase implies a role in tip growth and movement of the generative cell in pollen tubes. *The Plant Cell* **8,** 293–303.

Lindstrom, M. J. and Bates, D. M. (1990). Nonlinear mixed effects models for repeated measures data. *Biometrics* **46,** pp. 673–687.

Lions, P. L. (1982). On the existence of positive solutions of semilinear elliptic equations. *SIAM Review* **24,** 441–467.

Lowery, L. and Vanvactor, D. (2009). The trip of the tip: understanding the growth cone machinery. *Nature Reviews Molecular Cell Biology* **10,** 332–43.

Lu, C. J. and Meeker, W. Q. (1993). Using degradation measures to estimate a time-to-failure distribution. *Technometrics* **35,** pp. 161–174.

Lu, T., Liang, H., Li, H., and Wu, H. (2011). High dimensional odes coupled with mixed-effects modeling techniques for dynamic gene regulatory network identification. *Journal of the American Statistical Association* **106,** 1242–1258.

McKenna, S., Kunkel, J., Bosch, M., Rounds, C., Vidali, L., Winship, L., and Hepler, P. (2009). Exocytosis precedes and predicts the increase in growth in oscillating pollen tubes. *Plant Cell* **21,** 3026–3040.

Miao, H., Xia, X., Perelson, A., and Wu, H. (2011). On identifiability of nonlinear ode models with application in viral dynamics. *SIAM Review* **53,** 3–39.

Nelder, J. A. and Mead, R. (1965). A Simplex Method for Function Minimization. *The Computer Journal* **7,** 308–313.

Putter, H., S. H. Heisterkamp, J. M. A. L., and de Wolf, F. (2002). A bayesian approach to parameter estimation in hiv dynamical models. *Statistics in Medicine* **21,** 2199–2214.

Qin, Y. and Yang, Z. (2011). Rapid tip growth: insights from pollen tubes. *Seminars in Cell and Developmental Biology* **22,** 816–824.

Ramsay, J. O., Hooker, G., Campbell, D., and Cao, J. (2007). Parameter estimation for differential equations: a generalized smoothing approach. *Journal of the Royal Statistical Society: Series B (Statistical Methodology)* **69,** 741–796.

Soetaert, K. (2009). *rootSolve: Nonlinear root finding, equilibrium and steady-state analysis of ordinary differential equations.* R package 1.6.

Soetaert, K., Petzoldt, T., and Setzer, R. W. (2010). Solving differential equations in r: Package desolve. *Journal of Statistical Software* **33,** 1–25.

Wang, J. (1996). Asymptotics of Least-Squares Estimators for Constrained Nonlinear Regression. *The Annals of Statistics* **24,** 1316–1326.

Wolfinger, R. and Lin, X. (1997). Two taylor-series approximation methods for nonlinear mixed models. *Computational Statistics and Data Analysis* **25,** 465–490.

Wu, H. and Chen, J. (2008). Estimation of time-varying parameters in deterministic dynamic models. *Journal of the American Statistical Association* **103,** 369–384.

Xue, H., Miao, H., and Wu, H. (2010). Sieve estimation of constant and time-varying coefficients in nonlinear ordinary differential equation models by considering both numerical error and measurement error. *Annals of statistics* **38,** 2351–2387.

Yang, M. A.-Z. S. (2001). An approximate em algorithm for nonlinear mixed effects models. *Biometrical Journal* **43,** 881–893.

Yang, Z. (1998). Signaling tip growth in plants. *Current Opinion in Plant Biology* **1,** 523–530.

Yang, Z. (2008). Cell polarity signaling in Arabidopsis. *Annual Review of Cell and Developmental Biology* **24,** 551–575.